

---

# Effects of the Attenuation Map Used in the Chang Algorithm on Quantitative SPECT Results

ZongJian Cao and Lawrence E. Holder

Department of Diagnostic Radiology, University of Maryland Medical Center, Baltimore, Maryland

---

**Objective:** This study examined the effects on SPECT quantitation caused by erroneous size and position of the attenuation map and inaccurate pixel size used in the Chang algorithm.

**Methods:** Projection data of a three-dimensional head phantom were simulated with a uniform attenuation coefficient of 0.15/cm for the inside of the phantom. Images were reconstructed using the filtered backprojection algorithm without attenuation compensation and the Chang algorithm with different attenuation maps. Quantitative comparison then was performed between the reconstructed images and the phantom.

**Results:** The pixel values obtained for noisy data by using the first-order Chang algorithm with an accurate attenuation map were less than 10% different from the true values and the left-right asymmetry was under 5%. Small errors in the geometric parameters of the attenuation map, however, caused considerable quantitative inaccuracy in the reconstructed image. For example, a 0.64-cm error in the size of the map caused 10% deviation from the true value and a 0.64-cm shift of the position of the map towards the left produced 10% left-right pixel value asymmetry.

**Conclusion:** The accuracy of the Chang algorithm critically depends on the geometric parameters. For a uniform attenuator with symmetric geometry, such as the human brain, a true left-right symmetry in the pixel value can be altered significantly by a small error in the geometric parameters, while symmetry can be maintained with no attenuation compensation.

**Key Words:** SPECT; image reconstruction; attenuation compensation

*J Nucl Med Technol* 1998; 26:178-185

---

Quantitative results are demanded increasingly in nuclear medicine. Most of the available quantification protocols generate an average pixel value in a user-defined region of interest (ROI). The average pixel value then is compared among a series of sequential images (e.g., in renal studies), compared to

a normal database (e.g., in cardiac studies) or compared between two ROIs that are symmetrically located on the left and right sides of the image (e.g., in brain studies). The accuracy and precision of the quantitative results depend on both data acquisition and image reconstruction.

Photon attenuation is a major factor that degrades nuclear medicine images and introduces errors in quantitative analysis. To compensate for attenuation in SPECT reconstruction, several techniques have been developed (1-6). The Chang algorithm (7,8) is widely used in brain SPECT reconstruction to compensate for attenuation effects, due mainly to its high computational efficiency. Theoretically, the Chang algorithm can provide a good approximation for a distributed source located in a uniform attenuator such as the human head. The degree of approximation for uniform and nonuniform attenuators has been investigated (9-11) and is not the topic of this work.

In clinical practice, inaccurate geometric parameters (the size and position of the attenuation map and the pixel size) are often used with the Chang algorithm when attempting to compensate for photon attenuation. Little discussion can be found in the literature concerning the quantitative effects of inaccurate geometric parameters on the SPECT results. The purpose of this study was to investigate the quantitative effects of inaccurate geometric parameters used in the Chang algorithm for a uniform attenuator. We also examined the quantitative errors caused by attenuation and the improvement provided by the Chang algorithm with accurate geometric parameters. The quantitative investigation was performed by comparing selected profiles and average pixel values of several ROIs obtained from the reconstruction methods to the true values (absolute quantification). The average pixel values were compared between two selected ROIs that were located symmetrically on the left and right sides of the phantom (relative quantification), which is often used in brain SPECT.

## MATERIALS AND METHODS

### The Chang Algorithm

The Chang algorithm was developed as a postreconstruction iterative method for attenuation compensation in SPECT reconstruction (7,8). It requires an attenuation map that contains

---

For correspondence or reprints contact: ZongJian Cao, PhD, Department of Diagnostic Radiology, University of Maryland Medical Center, 22 South Greene St., Baltimore, MD 21201-1595.

the attenuation coefficient for each pixel in the image space. The first-order Chang algorithm that has been used most often in clinical practice can be performed in the following four steps:

1. Reconstruct the initial image  $I^0$  from the attenuated projection data  $P$  using the conventional filtered backprojection (FBP) algorithm.
2. Reproject the initial image with attenuation to generate the reprojection data  $R$ .
3. Compare the reprojection data  $R$  with the acquired data  $P$  and to reconstruct an image  $\Delta I^0$  from the difference  $(P - R)$  using the FBP algorithm.
4. Obtain the updated image  $I^1$  by adding the weighted difference image  $\Delta I^0/W$  to the initial image  $I^0$ , i.e:

$$I^1 = I^0 + \Delta I^0/W$$

in which the weighting factor  $W$  is calculated from the attenuation map.

These steps can be repeated to a preset iteration number  $N$ . The iteration number  $N$  of the first-order Chang algorithm is 1. In performing the second-order Chang algorithm ( $N = 2$ ), Steps 2–4 are performed twice. The initial image for the second iteration is the updated image from the first iteration ( $I^1$ ), and the updated image from the second iteration is  $I^2 = I^1 + \Delta I^1/W$ . Theoretically, the accuracy of a noise-free reconstructed image can be improved with more iterations. In practice, however, noise of the reconstructed image is amplified when the iteration continues. After a few iterations, the image may even become divergent. As a result, only the first-order or, at most, the second-order Chang algorithm has been applied in clinical practice.

### Simulation of the Projection Data

We simulated a three-dimensional Shepp-Logan head phantom that was composed of 14 ellipsoids of different size, position, orientation and activity concentration (12). The largest ellipsoid that defined the outline of the phantom had the dimensions of 15.43 (W)  $\times$  20.57 (L)  $\times$  27.09 (H) pixels.

Most of the investigation was done with noise-free projection data to demonstrate clearly the errors caused by an inaccurate attenuation map. The noise-free data were generated using an analytical method including photon attenuation (13) with 64 views over 360° and a 64  $\times$  64 matrix for each view. The pixel size was 0.64 cm. A constant attenuation coefficient of 0.15/cm was used for the inside of the phantom and no attenuation outside the phantom. In other words, the attenuator was a uniform ellipsoid coincident with the outline of the head phantom. Other degradation factors, such as photon scatter and spatially variant blurring, were not included since the purpose of this study was to investigate the accuracy of attenuation compensation. Without including scatter in the simulation, the attenuation coefficient for the 140-keV photons in water is 0.15/cm.

Noise properties of the reconstructed image resulting from the Chang algorithm vary with the increasing iteration even when a noise-free attenuation map is used. Although we did not attempt to investigate noise propagation of the Chang algorithm in this study, we wanted to examine whether image noise causes any changes in the errors of an inaccurate attenuation map from the noise-free reconstruction. Therefore, we simulated one set of noisy data that combined all possible errors of the attenuation map (see the next section). Noisy data were obtained by adding the random Poisson noise to the noise-free data (14). The noise level was determined by the total number of counts in the three-dimensional data. We used 5 million counts which is typical in brain SPECT.

### Possible Errors of the Attenuation Map

The Chang algorithm is a slice-by-slice reconstruction algorithm with attenuation compensation. It needs a two-dimensional attenuation map for correcting attenuation in each slice of the image. All the two-dimensional attenuation maps form a three-dimensional attenuation map. To avoid errors in the reconstructed image, the three-dimensional attenuation map used for the Chang algorithm should be exactly the same as the actual attenuator that is the patient's head (an approximate ellipsoid) in brain SPECT or the largest ellipsoid of the head phantom in this study. In practice, however, the attenuation map may deviate from the actual attenuator. The possible errors to an ellipsoid attenuator include:

1. Instead of the ellipsoid, a cylinder with the cross section determined by the largest transverse slice of the attenuator is used as the three-dimensional attenuation map for the Chang algorithm;
2. The major axis of the three-dimensional attenuation map (always the axis of rotation) is not coincident with that of the actual attenuator that may be tilted as shown in Figure 1; and/or
3. The pixel size of the attenuation map is not accurate.

The first two errors result in inaccurate two-dimensional attenuation maps used in the slice-by-slice reconstruction. Since the patient's head is best described as an ellipsoid, the cross section of the cylindrical attenuation map is accurate only for the largest transverse slice and is too large for other slices of the head. Also, the patient's head may be tilted with respect to the axis of rotation (Fig. 1). The tilt causes misplaced position and erroneous size of the two-dimensional attenuation map. The pixel size varies with different SPECT cameras and needs to be measured carefully using a well defined point source. We found the pixel sizes given by the vendors often deviated from the actual measured values. Since the pixel size is used to convert the attenuation coefficient for 1 cm into the attenuation coefficient for 1 pixel, the error in pixel size is passed on to the attenuation coefficient used in the reconstruction and affects the accuracy of the reconstructed image. The possible errors and sources of the errors are summarized in Table 1.

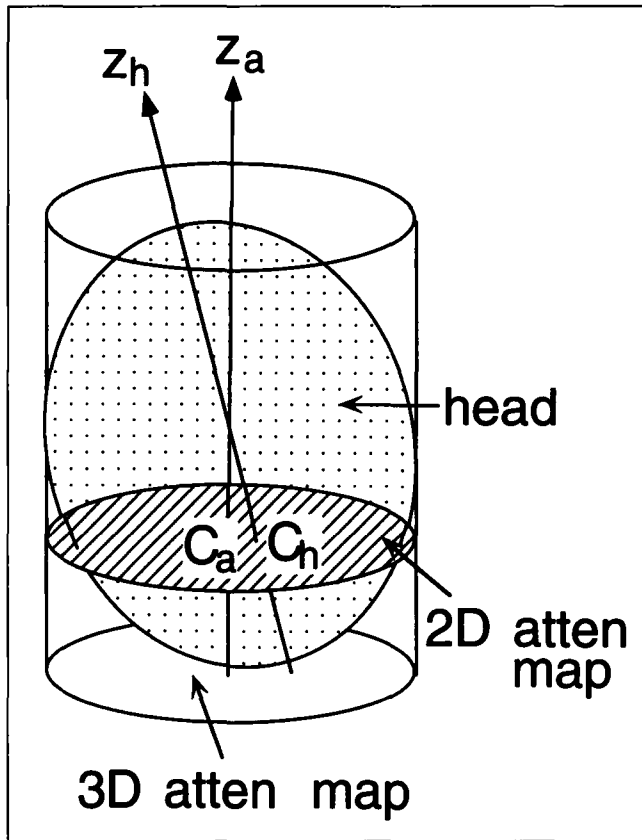


**FIGURE 1.** A schematic of a three-dimensional head phantom and a cylindrical attenuation map often used in brain SPECT. The cross section of the cylinder is the same as the largest slice of the head but is too large for other slices. If the axis of the head ( $Z_h$ ) is tilted with respect to the vertical axis of the cylinder ( $Z_a$ ), the center of the two-dimensional attenuation map ( $C_a$ ) is not coincident with the center of the head slice ( $C_h$ ).

As an example, a two-dimensional uniform attenuation map that was coincident with the outline of a slice of the head phantom was selected as shown in Figure 2. It was an ellipse with the semiaxes of 14.4 pixel ( $R_x$ ) and 19.3 pixel ( $R_y$ ) along the x and y axes, respectively. To investigate the effects of the

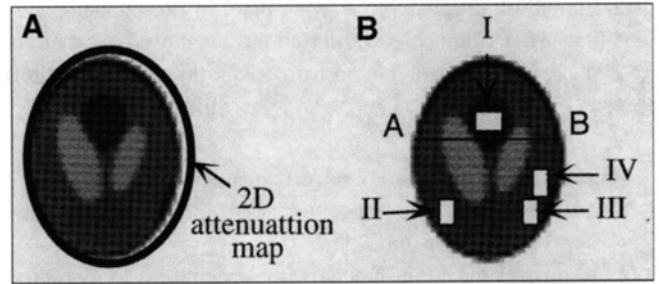


**FIGURE 2.** (A) The erroneous attenuation map and (B) the regions of interest examined in this study.

size of the attenuation map, we used three erroneous attenuation maps of the selected slice:  $R_x=13.4$  pixels and  $R_y=18.3$  pixels (smaller),  $R_x=15.4$  pixels and  $R_y=20.3$  pixels (larger), and  $R_x=16.4$  pixels and  $R_y=21.3$  pixels (even larger). Also, we shifted the center of the ellipse of  $R_x=16.4$  pixels and  $R_y=21.3$  pixels toward the left by 1 and 2 pixels relative to the head slice (Fig. 2A) to examine the effects of the position of an attenuation map. In addition, two erroneous values of the pixel size (0.58 cm and 0.70 cm) with  $\pm 10\%$  deviation from the exact value (0.64 cm) were used to study the effects of the pixel size.

The variation of the geometric parameters were applied separately to the noise-free data and the effects of a single erroneous geometric parameter were investigated. A realistic clinical situation also was examined in which image noise (with total counts of 5 million) was combined with a larger attenuation map ( $R_x=15.4$  and  $R_y=20.3$  pixels), 1 pixel (0.64 cm) off the center of the map, and a larger pixel size (0.70 cm).

### Quantitative Analysis

Both the FBP algorithm without attenuation compensation and the Chang algorithm were used for noise-free and noisy image reconstruction. For noisy data, we used the Butterworth filter with a fourth order and 0.2/pixel critical frequency to reduce image noise. The reconstructed images were normalized to the same total counts as the phantom and then compared to each other. The comparison was done for the average pixel value ( $\bar{p}$ ) and standard deviation ( $d$ ) of a selected ROI, which are defined as:

$$\bar{p} = \frac{1}{N} \sum_{i=1}^N p_i, \quad \text{and} \quad d = \sqrt{\frac{1}{N-1} \sum_{i=1}^N (p_i - \bar{p})^2}. \quad \text{Eq. 1}$$

Here  $N$  is the total number of pixels in the ROI and  $p_i$  is the  $i$ 'th pixel value. The ratio of the standard deviation to the average pixel value, in other words the coefficient of variation,  $d/\bar{p}$ , is an indication of the extent of fluctuation of pixel values.

Four uniform ROIs were chosen as shown in Figure 2B. The true pixel value in Region I was 77.83 and the area was  $7 \times 5$  pixels. Regions II and III were located symmetrically on the right and left sides of the slice, and had the same area ( $4 \times 7$  pixels) and true pixel value (52.93). These two ROIs were chosen to examine the left-right symmetry of the average pixel values. Region IV was located 3 pixels to the left and 7 pixels to the anterior relative to Region III with the same area ( $4 \times$

**TABLE 1**  
**Possible Errors of the Two-Dimensional Attenuation Maps Used for the Patient's Head**

Errors of two-dimensional attenuation maps	Sources of errors
Wrong shape	Use of a cylinder instead of an ellipsoid. Tilted major axis of the ellipsoid.
Inaccurate dimensions	Use of a cylinder instead of an ellipsoid. Tilted major axis of the ellipsoid.
Misplacement	Tilted major axis of the ellipsoid.
Inaccurate attenuation coefficient	Inaccurate pixel size.

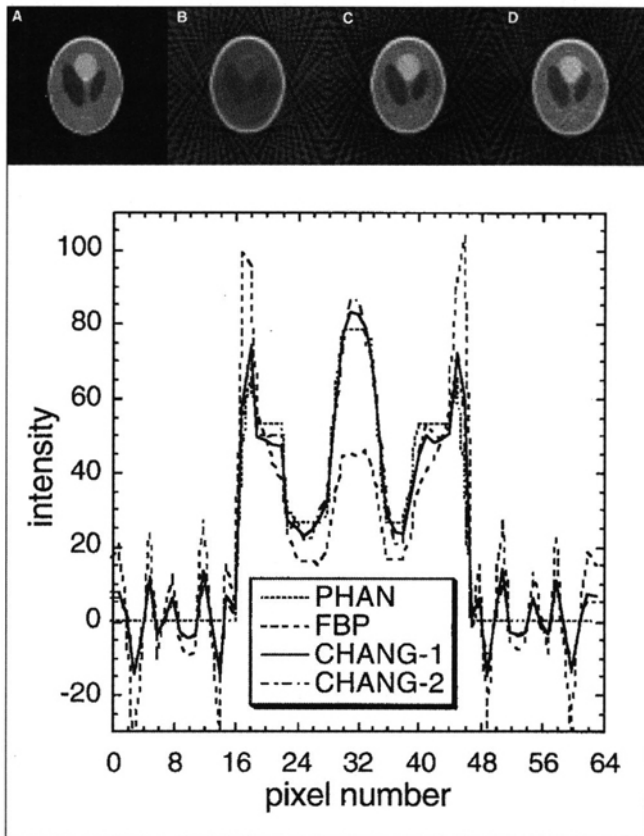


**FIGURE 3.** A selected slice of noise-free images obtained from (A) the phantom (PHAN), (B) the reconstruction without attenuation compensation (FBP), (C) the first-order Chang algorithm (CHANG-1) and (D) the second-order Chang algorithm (CHANG-2). The profiles were plotted along the line illustrated in Figure 2B, obtained from the images A, B, C and D.

7 pixels) and true pixel value (52.93). Regions II and IV were used to evaluate the asymmetry of the pixel values which was caused by the two slightly asymmetric ROI positions. In addition, the profile along the line AB in Figure 2B provided an

intuitive comparison of the pixel values and left-right symmetry.

## RESULTS

### Noise-Free Reconstruction With and Without Attenuation Compensation

Without attenuation compensation, the central region of the reconstructed image in Figure 3B was darker and the area near the edge was brighter than the phantom in Figure 3A. The details in the central region barely were perceptible due to the poor contrast. The first-order Chang algorithm made the central region brighter and better contrasted so that the details were observed more clearly as displayed in Figure 3C. The second-order Chang algorithm did not further reduce the attenuation effects, but produced more artificial pattern in the background (Fig. 3D).

The difference between the average pixel value and true value was less than 7% as a result of applying the Chang algorithm (Table 2). The difference between the first-order and second-order Chang algorithm was less than 2%. The left-right symmetry of average values was well preserved no matter whether with or without attenuation compensation. The difference of pixel values between Regions II and III was less than 1% in all images. The slightly increased difference between Regions II and IV was due to the small asymmetry in the position of the two ROIs.

### Noise-Free Reconstruction Using the Chang Algorithm with Inaccurate Geometric Parameters

As shown in Figure 4 and Table 3, the average pixel values of all ROIs resulting from a larger (or smaller) attenuation map were increased (or decreased). By changing 1 pixel in the semiaxis of the ellipse, the resultant pixel value changed by approximately 10%. However, the left-right symmetry of pixel values was maintained with a difference of less than 1%.

The shift of the position of the attenuation map towards the left, relative to the head slice, resulted in a darker region on

**TABLE 2**  
Average Pixel Values for Noise-Free Images Obtained Using the Filtered Backprojection Algorithm Without Attenuation Compensation, the First-Order Chang Algorithm and the Second-Order Chang Algorithm

Algorithm	Without compensation		First-order Chang		Second-order Chang	
	Average	Difference (%) <sup>*</sup>	Average	Difference (%)	Average	Difference (%)
Region I	51.10	-34.35	79.38	1.99	79.05	1.56
Region II	47.13	-10.95	50.31	-4.94	51.16	-3.33
Region III	47.25	-10.72	50.42	-4.73	51.26	-3.15
Difference of II and III <sup>**</sup> (%)	-0.25	—	-0.22	—	-0.20	—
Region IV	45.89	-13.29	49.56	-6.36	50.19	-5.17
Difference of II and IV <sup>**</sup> (%)	2.67	—	1.50	—	1.91	—

<sup>\*</sup>Defined as  $\frac{\text{Pixel value} - \text{true value}}{\text{True value}} \cdot 100\%$ .

<sup>\*\*</sup>Defined as  $\frac{\text{Difference of pixel values in the two ROIs}}{\text{Average of pixel values in the two ROIs}} \cdot 100\%$ .

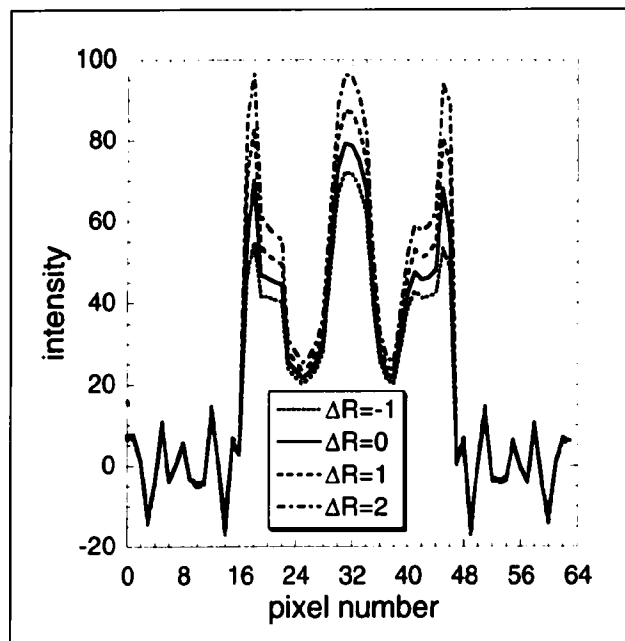


**FIGURE 4.** Noise-free profiles obtained using different sizes of the attenuation map. The profiles were plotted along the line illustrated in Figure 2B. The dotted ( $\Delta R = -1$ ), solid ( $\Delta R = 0$ ), dashed ( $\Delta R = 1$ ) and dot-dashed ( $\Delta R = 2$ ) lines represent the profiles obtained with 1 pixel less than the head slice, with the same size of the slice, with 1 pixel larger than the slice, and with 2 pixels larger than the slice.

the right side and a brighter region on the left side of the images as shown in Figure 5B (1-pixel shift) and more prominently in Figure 5C (2-pixel shift). The difference in average pixel values for Regions II and III was 13.44% with a 1-pixel shift and 26.15% with a 2-pixel shift (Table 4).

When the pixel size is 10% off the true size, the average pixel values are erroneously changed by ~5% (Table 5). These errors mostly occurred in the central region (Region I). However, the left-right symmetry in pixel values was preserved (Fig. 6).

#### Noisy Reconstruction Using the Chang Algorithm with Inaccurate Geometric Parameters

With inaccurate geometric parameters (a 1-pixel larger attenuation map with its center shifted by 1 pixel to the left and

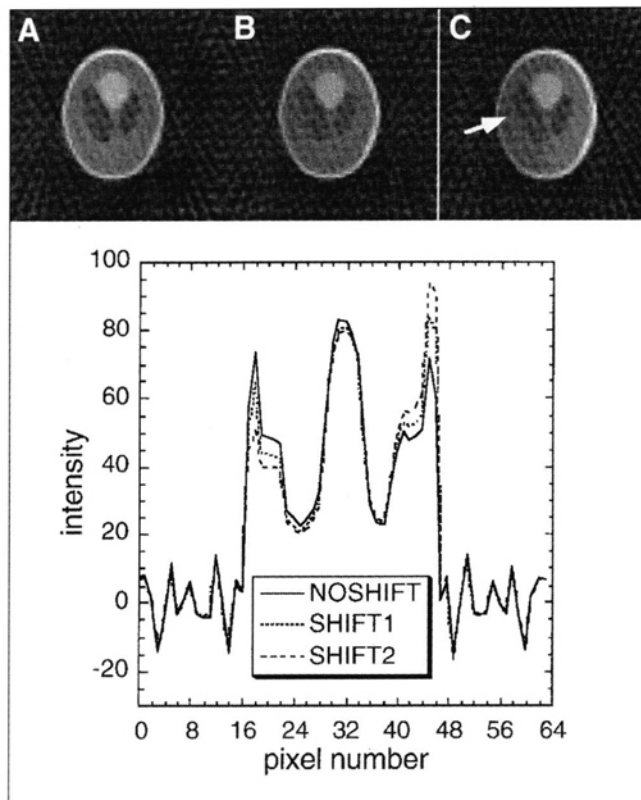


**FIGURE 5.** A selected slice of noise-free images obtained using the first-order Chang algorithm with the center of the attenuation map located at (A) the center of the head slice, (B) 1 pixel to the left of the center of the slice and (C) 2 pixels to the left of the center of the slice. The profiles were plotted along the line illustrated in Figure 2B for image A (NOSHIFT), image B (SHIFT1) and image C (SHIFT2).

with a 10% larger pixel size), the right side of the image (Fig. 7B) appeared darker than the left side. The quantitative results (Table 6) demonstrated that left-right symmetry was destroyed by the erroneous geometric parameters. The difference of average pixel values for Regions II and III was 14.67%.

#### DISCUSSION

Without attenuation compensation, the deviations of pixel values from the true values are significant and vary with the

**TABLE 3**  
Average Pixel Values for Noise-Free Reconstructed Images Obtained from the First-Order Chang Algorithm with Different Sizes of the Attenuation Map

Size of map	X = 13.4, Y = 18.3		X = 14.4, Y = 19.3*		X = 15.4, Y = 20.3		X = 16.4, Y = 21.3	
	Average	Difference (%)	Average	Difference (%)	Average	Difference (%)	Average	Difference (%)
Region I	72.08	-7.39	79.38	1.99	87.69	12.67	97.01	24.64
Region II	45.15	-14.69	50.31	-4.94	56.47	6.70	63.38	19.75
Region III	45.36	-14.29	50.42	-4.73	56.47	6.70	63.49	19.96
Difference of II and III (%)	-0.46	—	-0.22	—	0.00	—	-0.17	—
Region IV	44.56	-15.81	49.56	-6.36	55.71	5.25	62.77	18.60
Difference of II and IV (%)	1.32	—	1.50	—	1.36	—	0.97	—

\*Actual size of the attenuation map used in the simulation.

**TABLE 4**  
**Average Pixel Values for Noise-Free Reconstructed Images Obtained from the First-Order Chang Algorithm with a Shifted Attenuation Map Towards the Left by One and Two Pixels**

Shift of map center	0 pixel		1 pixel		2 pixels	
	Average	Difference (%)	Average	Difference (%)	Average	Difference (%)
Region I	97.01	24.64	94.63	21.58	94.33	21.20
Region II	63.38	19.75	58.30	10.16	54.46	2.90
Region III	63.49	19.96	66.70	26.03	70.84	33.86
Difference of II and III (%)	-0.17	—	-13.44	—	-26.15	—
Region IV	62.77	18.60	66.58	25.81	71.50	35.09
Difference of II and IV (%)	0.97	—	-13.26	—	-27.05	—

location of the ROI. For example, there is a 34% error in the central region and only 11% in a region near the edge of the attenuator. This is because the photons emitted from the center travel a longer distance in the attenuator and experience more attenuation than those emitted from the edge. However, the difference in pixel values between two ROIs that are located symmetrically on the left and right sides of a uniform elliptical attenuator (e.g., Regions II and III) is rather small even without attenuation compensation, since the photons emitted from the two ROIs are subject to similar attenuation. If only the difference between two symmetrically located ROIs is of interest, then compensation for attenuation may not be necessary.

For a uniform attenuator, the Chang algorithm improves the visual quality and, more critically, improves the quantitative accuracy. The first-order Chang algorithm with an accurate attenuation map can provide an absolute accuracy of better than 7% of the true pixel value within a uniform ROI. The left-right symmetry in pixel values also is well preserved. The second-order Chang algorithm is not recommended since it produces little improvement in accuracy, while generating more artifacts than the first-order Chang algorithm.

However, a small error in the size of the attenuation map may affect considerably the accuracy of absolute quantification. If the attenuation map is larger or smaller than the actual attenuator by 1 pixel, the resultant pixel value is larger (over compensation) or smaller (under compensation) by ~10% than the results obtained from using an accurate attenuator.

The over compensation resulting from using a 1-pixel larger attenuation map can be explained by:

$$e^{0.15/\text{cm} \cdot 0.64\text{cm}} = 1.10 \quad \text{Eq. 2}$$

Here the 0.15/cm is the attenuation coefficient in water and 0.64 cm is the pixel size. It should be noted that the ratio of the pixel values between two symmetrically located ROIs remains the same due to the cancellation of the increased (or decreased) factors. Therefore, the left-right symmetry can be preserved even when an erroneous size is used for the attenuation map.

The misplacement of the attenuation map produces different compensation for different locations. For a central ROI, such as Region I, little change in the pixel value is observed (less than 3%), while near the edge, such as Region II or III, the change is significant. Moreover, the change is different along different directions, resulting in an appreciable asymmetry in average pixel values. This difference can be explained by the ratio of the distance to the boundary of the attenuation map versus the distance to the boundary of the actual attenuator. Since the distance from Region I to the boundary is quite large, the ratio does not change much as a result of a 1- or 2-pixel shift of the position of the attenuation map. For a region near the edge, such as Region II, the distance to the right edge of the attenuator is rather small (Fig. 2A), so a 1- or 2-pixel decrease causes a large decrease in the ratio of the distances. For Region III, the same argument applies, but the

**TABLE 5**  
**Average Pixel Values for Noise-Free Reconstructed Images Obtained from the First-Order Chang Algorithm with Different Pixel Sizes**

Pixel size (mm)	5.80		6.4*		7.00	
	Average	Difference (%)	Average	Difference (%)	Average	Difference (%)
Region I	75.50	-3.00	79.38	1.99	83.43	7.19
Region II	50.16	-5.22	50.31	-4.94	50.38	-4.81
Region III	50.27	-5.02	50.42	-4.73	50.49	-4.60
Difference of II and III (%)	-0.22	—	-0.22	—	-0.22	—
Region IV	49.79	-5.92	51.12	-3.41	53.42	0.93
Difference of II and IV (%)	0.74	—	-1.60	—	-5.86	—

\*Actual pixel size used in the simulation.

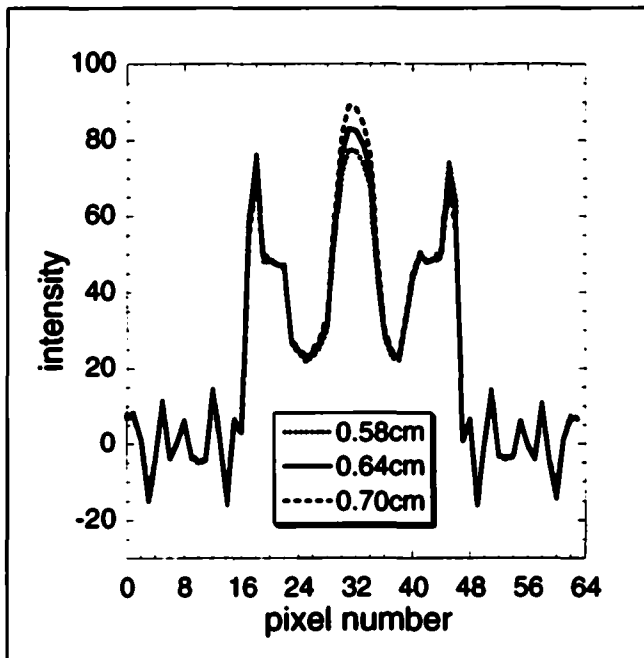


**FIGURE 6.** Noise-free profiles obtained using the first-order Chang algorithm with different pixel sizes. The profiles were plotted along the line illustrated in Figure 2B. The dotted, solid and dashed lines represent the profiles obtained with 0.58 cm, 0.64 cm (exact) and 0.70 cm.

ratio of the distance is increased. Thus, the difference for Regions II and III is even larger. As a result, a misplacement of the position of the attenuation map by only 1 pixel severely degrades the accuracy of both absolute and relative quantification for a ROI near the boundary of the attenuator.

The exact attenuation coefficient over 1 pixel is  $0.096/\text{pixel}$  ( $=0.15/\text{cm} \times 0.64 \text{ cm}/\text{pixel}$ ) in the simulation. A smaller or larger pixel value produces a smaller or larger attenuation coefficient for 1 pixel, resulting in under or over compensation. This is why the average pixel value decreases or increases with a smaller or larger pixel size. The effects are most prominent for a central ROI, such as Region I, since it has a larger average distance to the boundary of the attenuation map.

In reality, all degradation factors simultaneously play roles in image reconstruction. A simple but crude method to compensate for photon scatter is to decrease the attenuation coefficient, for example, from  $0.15/\text{cm}$  to  $0.12/\text{cm}$  for 140-keV photons in water. However, most modern scatter compensation methods use more sophisticated approaches and thus provide more accurate compensation. These methods are not related to attenuation compensation, so that the errors resulting from scatter compensation are independent of the errors that are examined in this study. We believe that the results obtained using the attenuation coefficient of  $0.15/\text{cm}$  in this study is in the interest of a more accurate SPECT reconstruction.

Usually, brain SPECT is performed with 128 views over  $360^\circ$  and a  $128 \times 128$  matrix for each view. In this study, however, we used 64 views and a  $64 \times 64$  matrix each view to reduce image noise and thus decrease fluctuations of the numerical results. For noise-free reconstruction, the effects of 1-pixel

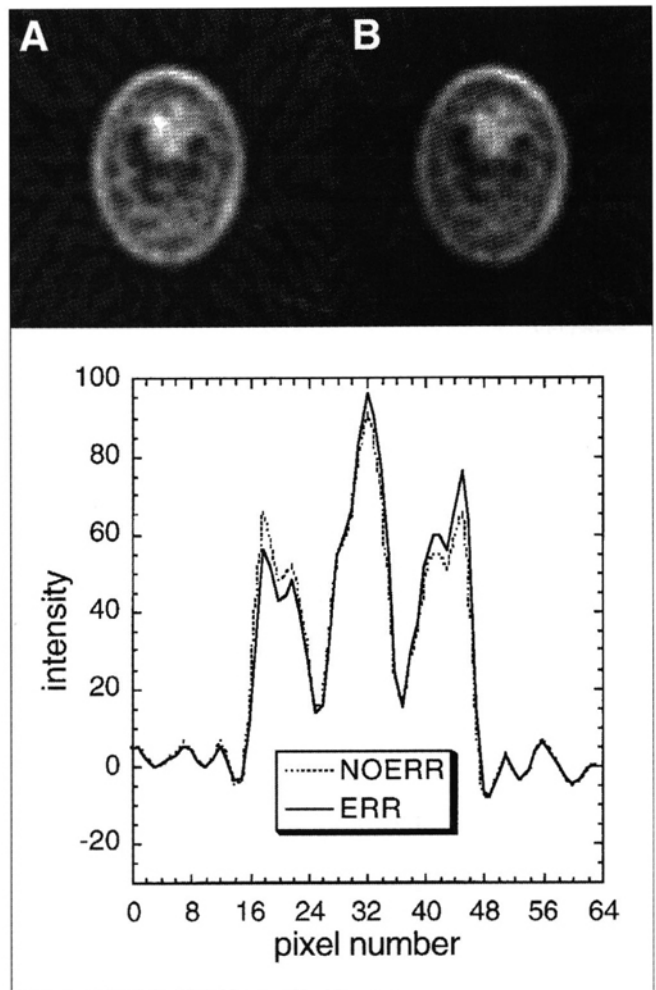


**FIGURE 7.** A selected slice of noisy images obtained using the first-order Chang algorithm with (A) accurate geometric parameters and (B) erroneous geometric parameters. The profiles were plotted along the line illustrated in Figure 2B, obtained from the image A (NOERR) and image B (ERR).

shift or 1-pixel deviation in size for a  $64 \times 64$  image are the same as those of a 2-pixel shift or 2-pixel deviation in size for a  $128 \times 128$  image with the same field of view. For noisy reconstruction, the effects are similar but not exactly the same due to different noise properties. In any case, the effects of a 1-pixel shift or 1-pixel deviation in size for a  $128 \times 128$  image is less prominent than those for a  $64 \times 64$  image.

For noisy projection data, if the geometric parameters are not accurate, artifacts are clearly seen in the reconstructed image and the accuracy of both absolute and relative quantification is degraded. In particular, a small shift (e.g., 1 pixel) in the position of the attenuation map can cause a larger than 10% error in the average pixel values for two symmetrically located ROIs, which may mislead to a false abnormality in brain studies.

## CONCLUSION

For noisy reconstruction with a uniform attenuator, the difference between the average pixel value obtained from the

**TABLE 6**  
**Average Counts and Standard Deviation for Noisy Reconstructed Images Obtained from the First-Order Chang Algorithm with Accurate Parameters and with Erroneous Parameters\***

Algorithm	Accurate Chang			Erroneous Chang		
	Average (p)	Difference (%)	d/p (%)	Average (p)	Difference (%)	d/p (%)
Region I	82.45	5.93	9.31	87.65	12.61	9.01
Region II	47.92	-9.46	18.26	41.30	-21.97	18.55
Region III	48.02	-9.27	11.91	47.84	-9.61	13.34
Difference of II and III (%)	-0.21	—	—	-14.67	—	—
Region IV	46.06	-12.97	18.87	49.74	-6.02	19.32
Difference of II and IV (%)	3.96	—	—	-18.54	—	—

\*The images were filtered using a 4th-order Butterworth filter of 0.2/pixel critical frequency.

first-order Chang algorithm and the true value can be less than 10%. The left-right difference in average pixel values is less than 5%. The results indicate that adequate relative quantification can be achieved by using the Chang algorithm.

The accuracy of the Chang algorithm critically depends on geometric parameters (the size and position of the attenuation map and the pixel size). The misplacement of the position of the attenuation map may destroy the left-right symmetry. A 1-pixel off-center shift of the attenuation map can cause a larger than 10% asymmetry. Also, a 1-pixel error in the size of the attenuation map or a 10% error in the pixel size can cause 10% or 5% differences in the resultant pixel values.

If only the left-right comparison is concerned, attenuation compensation may not be necessary since the photons emitted from the two symmetrically located ROIs experience the same amount of attenuation. However, the conclusion cannot be extended to an attenuator that is not uniform or does not have a symmetric shape. In addition, it is not true for two ROIs that are not located symmetrically.

It is likely that the geometric parameters are also important in other attenuation compensation methods such as the often used iterative reconstruction algorithms. The errors in the parameters may cause similar effects as in the Chang algorithm, but further investigation is needed to verify this speculation. As demonstrated in this study, an inaccurate attenuation map causes errors in the reconstructed image, but use of an accurate attenuation map does not warrant accurate quantitation since the accuracy in SPECT also is affected by other degradation factors, such as photon scatter and spatially variant blurring. True accurate quantitation in SPECT can be achieved only after all the degradation factors are corrected appropriately.

#### ACKNOWLEDGMENT

This work was supported in part by National Cancer Institute Public Health Grant CA61039. The contents of this paper

are solely the responsibility of the authors and do not necessarily represent the official views of the National Cancer Institute.

#### REFERENCES

- Bellini S, Piacentini M, Cafforio C, et al. Compensation of tissue absorption in emission tomography. *IEEE Trans Acoust Speech Signal Proc* 1979;ASSP-27:213-218.
- Tretiak O, Metz CE. The exponential radon transform. *SIAM J Appl Math* 1980;39:341-354.
- Gullberg GT, Budinger TF. The use of filtering methods to compensate for constant attenuation in single-photon emission computed tomography. *IEEE Trans Biomed Eng* 1981;28:142-157.
- Inouye T, Kose K, Hasegawa A. Image reconstruction algorithm for single-photon emission computed tomography with uniform attenuation. *Phys Med Biol* 1989;34:299-304.
- Metz CE, Pan X. A unified analysis of exact methods of inverting the 2D exponential radon transform, with implications for noise control in SPECT. *IEEE Trans Med Imag* 1995;14:643-658.
- Pan X, Metz CE. Analysis of noise properties of a class of exact methods of inverting the 2D exponential radon transform. *IEEE Trans Med Imag* 1995; 14:659-668.
- Chang LT. A method for attenuation correction in radionuclide computed tomography. *IEEE Trans Nucl Sci* 1978;25:638-643.
- Manglos SH, Jaszczak RJ, Floyd CE, et al. Non-isotropic attenuation in SPECT: phantom tests of quantitative effects and compensation techniques. *J Nucl Med* 1987;28:1584-1591.
- Tsui BM, Gullberg GT, Edgerton ER, et al. Correction of nonuniform attenuation in cardiac SPECT imaging. *J Nucl Med* 1989;30:497-507.
- Liang Z, Ye J, Harrington DP. An analytical approach to quantitative reconstruction of non-uniform attenuated brain SPECT. *Phys Med Biol* 1994;39:2023-2041.
- Glick SJ, King MA, Pan TS, et al. Compensation for nonuniform attenuation in SPECT brain imaging. *IEEE Tran Nucl Sci* 1996;43:737-750.
- Shepp LA, Logan BF. The Fourier reconstruction of a head section. *IEEE Trans Nucl Sci* 1974;21:21-43.
- Cao ZJ, Tsui BMW. A fully three-dimensional reconstruction algorithm with the nonstationary filter for improved single-orbit cone beam SPECT. *IEEE Trans Nucl Sci* 1993;40:280-287.
- Press WH, Flannery BP, Teukolsky SA, et al. *Numerical recipes: the art of scientific computing*. New York: Cambridge University Press; 1986:206-208.